# Metallic $LiMo_3Se_3$ Nanowire Film Sensors for Electrical Detection of Metal Ions in Water

Mark Allen,[†] Erwin M. Sabio,[†] Xiubin Qi,[†] Bokuba Nwengela,[‡] M. Saif Islam,[‡] and Frank E. Osterloh*,[†]

*Departments of Chemistry, and Electrical and Computer Engineering, University of California, Davis, One Shields Avenue, Davis, California 95616*

*Received February 5, 2008. Revised Manuscript Received March 30, 2008*

$LiMo_3Se_3$ nanowire film sensors were fabricated by drop-coating a 0.05% (mass) aqueous nanowire solution onto microfabricated indium tin oxide electrode pairs. According to scanning electron microscopy (SEM) and atomic force microscopy (AFM), the films are made of a dense network of 3−7 nm thick nanowire bundles. Immersion of the films in 1.0 M aqueous solutions of group 1 or 2 element halides or of Zn(II), Mn(II), Fe(II), or Co(II) chlorides results in an increase of the electrical resistance of the films. The resistance change is always positive and reaches up to 9% of the base resistance of the films. It occurs over the course of 30−240 s, and it is reversible for monovalent ions and partially reversible for divalent ions. The signal depends on the concentration of the electrolyte and on the size and charge of the metal cation. Anions do not play a significant role, presumably, because they are repelled by the negatively charged nanowire strands. The magnitude of the electrical response and its sign suggest that it is due to analyte-induced scattering of conduction electrons in the nanowires. An ion-induced field effect can be excluded based on gated conductance measurements of the nanowire films.

## Introduction

Nanowire-based structures have been shown in recent years to exhibit superior performance as chemical sensors, both in terms of detection limits and in terms of time scale.[1–9] While most nanowire sensors are based on semiconductors, for example, silicon or carbon, some sensors are comprised of metallic nanostructures.[9–11] In 1998, Tao et al. showed that atomically thin Au nanowires created between a Au scanning tunneling microscopy (STM) tip and a gold surface responded to molecular adsorbates with a change of the quantum conductance.[12] This effect was attributed to increased scattering of the conduction electrons and to a distortion of the atomic arrangement in the nanowires casued by the analyte. Similar effects were later observed in electrochemically fabricated Cu nanowires.[11] Penner's group showed in 2001 that Pd microwires detect hydrogen gas down to a concentration of 1%.[9] Here, the sensing mechanism involves swelling of the Pd grains in the wire causing the disappearance of break junctions. Microwires of Pt, Cu, and Ag have similarly been used for the detection of ammonia.[13,14] In these cases, the analyte induced conductivity variations are attributed to semiconducting metal oxides that are present at the nanowire boundaries. Work in our laboratory has focused on sensors based on metallic nanowire films derived from the Chevrel phase $LiMo_3Se_3$.[15–19] Metallic films obtained by drop-coating nanowire solutions onto solid substrates can detect molecular analytes down to the parts per million (ppm) level.[18] In these films, the resistance increase is due to changes in the interwire charge transport resulting from coating of the nanowires by a nonconductive analyte film.[16] Here, we show that the same nanowire films can be adopted for the detection of metal ions in aqueous solution. The ability to detect metal ions in aqueous solution is significant for environmental monitoring, waste management, medicine, and other areas. Other detection schemes for metal ions involve electrochemical procedures, such as stripping voltammetry[20,21] or capacitance measurements,[22,23] but optical methods[23,24] and field effect transistors based on

* To whom correspondence should be addressed. Fax: (+1) 530 752 8995. Telephone: (+1) 530 752 6242. E-mail: fosterloh@ucdavis.edu.
† Department of Chemistry.
‡ Department of Electrical and Computer Engineering.

(1) Cui, Y.; Wei, Q. Q.; Park, H. K.; Lieber, C. M. *Science* **2001**, *293*(5533), 1289–1292.
(2) Kolmakov, A.; Moskovits, M. *Annu. Rev. Mater. Res.* **2004**, *34*, 151–180.
(3) Varghese, O. K.; Gong, D. W.; Paulose, M.; Ong, K. G.; Grimes, C. A. *Sens. Actuators, B* **2003**, *93*(1−3), 338–344.
(4) Wang, Z. L. *Adv. Mater.* **2003**, *15*(5), 432–436.
(5) Huang, J.; Virji, S.; Weiller, B.; Kaner, R. *J. Am. Chem. Soc.* **2003**, *125*(2), 314–315.
(6) Xia, Y. N.; Yang, P. D.; Sun, Y. G.; Wu, Y. Y.; Mayers, B.; Gates, B.; Yin, Y. D.; Kim, F.; Yan, Y. Q. *Adv. Mater.* **2003**, *15*(5), 353–389.
(7) Zheng, G. F.; Patolsky, F.; Cui, Y.; Wang, W. U.; Lieber, C. M. *Nat. Biotechnol.* **2005**, *23*(10), 1294–1301.
(8) Law, M.; Kind, H.; Messer, B.; Kim, F.; Yang, P. D. *Angew. Chem., Int. Ed.* **2002**, *41*(13), 2405–2408.
(9) Favier, F.; Walter, E. C.; Zach, M. P.; Benter, T.; Penner, R. M. *Science* **2001**, *293*(5538), 2227–2231.
(10) Bogozi, A.; Lam, O.; He, H. X.; Li, C. Z.; Tao, N. J.; Nagahara, L. A.; Amlani, I.; Tsui, R. *J. Am. Chem. Soc.* **2001**, *123*(19), 4585–4590.
(11) Li, C. Z.; He, H. X.; Bogozi, A.; Bunch, J. S.; Tao, N. J. *Appl. Phys. Lett.* **2000**, *76*(10), 1333–1335.
(12) Li, C. Z.; Sha, H.; Tao, N. J. *Phys. Rev. B* **1998**, *58*(11), 6775–6778.
(13) Murray, B. J.; Walter, E. C.; Penner, R. M. *Nano Lett.* **2004**, *4*(4), 665–670.
(14) Murray, B. J.; Newberg, J. T.; Walter, E. C.; Li, Q.; Hemminger, J. C.; Penner, R. M. *Anal. Chem.* **2005**, *77*(16), 5205–5214.
(15) Qi, X.; Osterloh, F. E.; Giacomo, J. A.; Chiang, S. *Langmuir* **2006**, *22*(19), 8253–8256.
(16) Qi, X.; Osterloh, F. E.; Barriga, S. A.; Giacomo, J. A.; Chiang, S. *Anal. Chem.* **2006**, *78*(4), 1306–1311.
(17) Akl, N. N.; Trofymluk, O.; Qi, X. B.; Kim, J. Y.; Osterloh, F. E.; Navrotsky, A. *Angew. Chem., Int. Ed.* **2006**, *45*(22), 3653–3656.
(18) Qi, X. B.; Osterloh, F. E. *J. Am. Chem. Soc.* **2005**, *127*(21), 7666–7667.
(19) Osterloh, F. E.; Martino, J. S.; Hiramatsu, H.; Hewitt, D. P. *Nano Lett.* **2003**, *3*(2), 125–129.
(20) Anderson, J. L.; Bowden, E. F.; Pickup, P. G. *Anal. Chem.* **1996**, *68*(12), R379–R444.
(21) Kovacs, G. T. A.; Storment, C. W.; Kounaves, S. P. *Sens. Actuators, B* **1995**, *23*(1), 41–47.
(22) Bontidean, I.; Berggren, C.; Johansson, G.; Csoregi, E.; Mattiasson, B.; Lloyd, J. A.; Jakeman, K. J.; Brown, N. L. *Anal. Chem.* **1998**, *70*(19), 4162–4169.
(23) Corbisier, P.; van der Lelie, D.; Borremans, B.; Provoost, A.; de Lorenzo, V.; Brown, N. L.; Lloyd, J. R.; Hobman, J. L.; Csoregi, E.; Johansson, G.; Mattiasson, B. *Anal. Chim. Acta* **1999**, *387*(3), 235–244.
(24) Forzani, E. S.; Zhang, H. Q.; Chen, W.; Tao, N. J. *Environ. Sci. Technol.* **2005**, *39*(5), 1257–1262.

10.1021/la8004085 CCC: $40.75 
Published on Web 05/29/2008

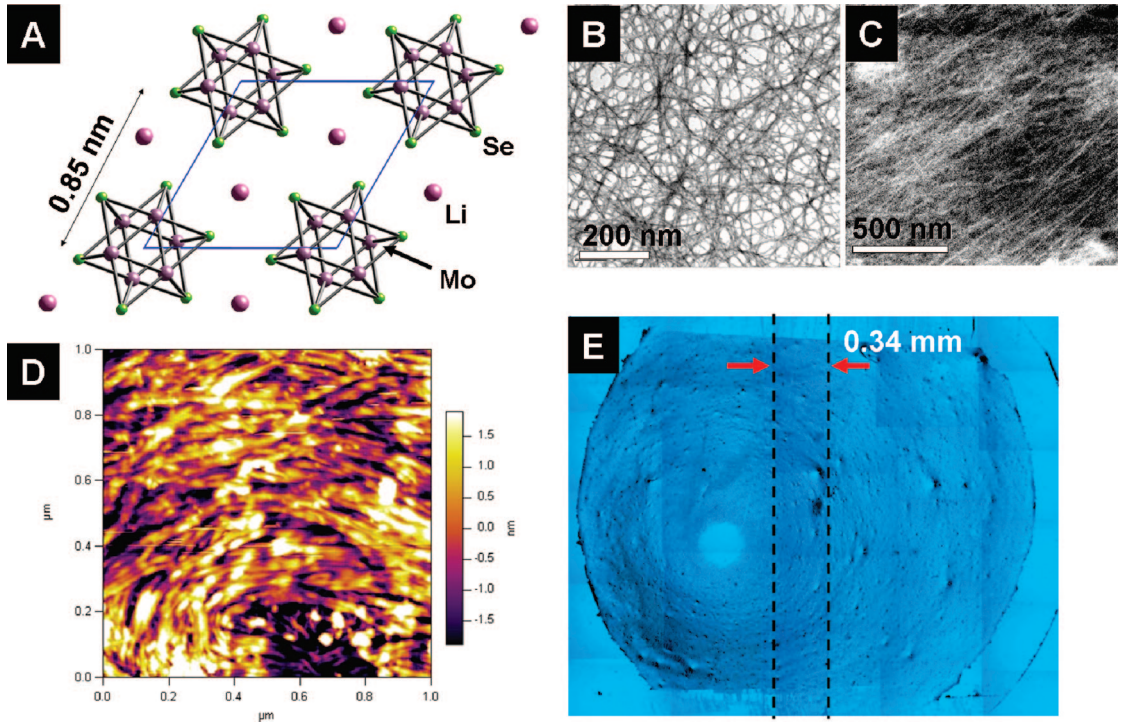


**Figure 1.** (A) Crystallographic structure of $LiMo_3Se_3$ viewed along the *c*-direction. (B) TEM image of a $LiMo_3Se_3$ nanowire film, dried from a 0.003% aqueous solution. (C) SEM image of a nanowire film. (D) AFM image of a $LiMo_3Se_3$ nanowire film. (E) Optical micrograph of a $LiMo_3Se_3$ nanowire film on top of two vertical ITO electrode fingers with the nonconductive gap indicated by dotted lines. Film edges on the top and bottom were cut off to minimize charge transport along film edges.

semiconducting films have also been employed.[25] The $LiMo_3Se_3$ nanowire film sensors presented here detect ions via a change of the electrical resistance. The resistance change is always positive, and its size is up to 9% of the base resistance of the films. It occurs over the course of 30−240 s, and it is reversible for monovalent ions and partially reversible for divalent ions. The signal depends on the concentration of the electrolyte and on the size and charge of the metal cation. Anions do not play a significant role, presumably, because they are repelled by the negatively charged nanowire strands.

## Experimental Section

Indium tin oxide (ITO) electrode arrays with 0.34 mm electrode spacing were prepared from ITO-coated (120−160 nm thick) aluminosilicate glass slides (1.1 mm thick, Delta Technologies) using a published lithographic technique.[26] Water was purified with a Nanopure system to a final resistivity of > 18 MΩ cm and deaerated with nitrogen gas before use. Elemental analysis were performed on a Cameca SX-100 electron microprobe system. Atomic force micrographs were obtained using the tapping mode on an Asylum Research MFP-3D microscope. BS-Tap300AI silicon nitride cantilevers from Budget Sensors with a resonant frequency of 300 kHz and a force constant of 40 N/m were used as probes. Transmission electron microscopy (TEM) data was obtained from a Philips CM12 microscope. Two-contact resistance measurements were made with a Keithley 2700 multimeter connected to a Microsoft Windows computer system.

**Synthesis of Exfoliated $LiMo_3Se_3$ Nanowires.** Solid $LiMo_3Se_3$ was prepared by a two-step solid-state synthesis via $InMo_3Se_3$ as the intermediate.[27,28] Cation exchange with LiI was performed under active vacuum. The identity of the resulting gray powder was confirmed by microprobe elemental analysis and scanning electron microscopy (SEM). A 0.05% (mass) solution of $LiMo_3Se_3$ nanowires was prepared by dissolving 5 mg of the solid in 10 g of pure (MΩ cm) water and by sonicating for 5 min. This solution was stored in a $N_2$ atmosphere. The exfoliated nanowires were characterized by transmission electron microscopy, atomic force microscopy, and microprobe analysis (see Results and Discussion).

**Preparation of Nanowire Films.** Small drops (∼2 mg) of $LiMo_3Se_3$ nanowire solution were deposited on the ITO electrode array, onto the 0.34 mm gaps between ITO fingers. The water was allowed to evaporate under $N_2$, producing submicrometer thick nanowire films. The slightly thicker edges of the dried film were removed manually with a razor blade. To strengthen the films, partial Li cation exchange was carried out by immersing the films for 10 min in aqueous 20% KBr solution, followed by rinsing with water. The final film composition was determined by microprobe elemental analysis to be $Li_{0.64}K_{0.36}Mo_3Se_3$.

**Analyte Detection.** The film-coated ITO electrode array was attached to a multimeter with the electrode array angled at ∼30°, allowing for the nanowire film portion to be drenched with water. Aliquots of 1.0 mM analyte solution and purified water were then alternately added to the film at 2 min intervals while resistance data was continually recorded. Selected alkali metal halides (MX, M = Li, Na, K, Rb, Cs; X = Cl, Br, I), alkaline earth halides ($MgCl_2$, $CaCl_2$, $SrCl_2$, $BaCl_2$), and divalent first row transition metal chlorides and sulfates ($MnCl_2$, $FeCl_2$, $CoCl_2$, $ZnCl_2$, $MnSO_4$, $FeSO_4$, $CoSO_4$, $ZnSO_4$) were freshly prepared before the measurements as 1.0 mM solutions.

## Results and Discussion

The Chevrel phase $LiMo_3Se_3$ consists of infinite $Mo_3Se_3$ cluster columns along the *c*-direction of the crystal (Figure 1A). The columns are built from triangular $Mo_3Se_3^-$ units that are interconnected by Mo−Mo and Mo−Se bonds. The negative charge of the cluster is compensated by lithium ions. Treatment of $LiMo_3Se_3$ with water results in exfoliated nanowire bundles

(25) Dzyadevych, S. V.; Soldatkin, A. P.; El'skaya, A. V.; Martelet, C.; Jaffrezic-Renault, N. *Anal. Chim. Acta* **2006**, *568*(1−2), 248–258.
(26) Hawatky, A.; Osterloh, F. E. *Instrum. Sci. Technol.* **2007**, *35*(1), 53–58.
(27) Tarascon, J. M.; DiSalvo, F. J.; Chen, C. H.; Carroll, P. J.; Walsh, M.; Rupp, L. *J. Solid State Chem.* **1985**, *58*, 290–300.
(28) Tarascon, J. M.; Hull, G. W.; DiSalvo, F. J. *Mater. Res. Bull.* **1984**, *19*, 915–924.

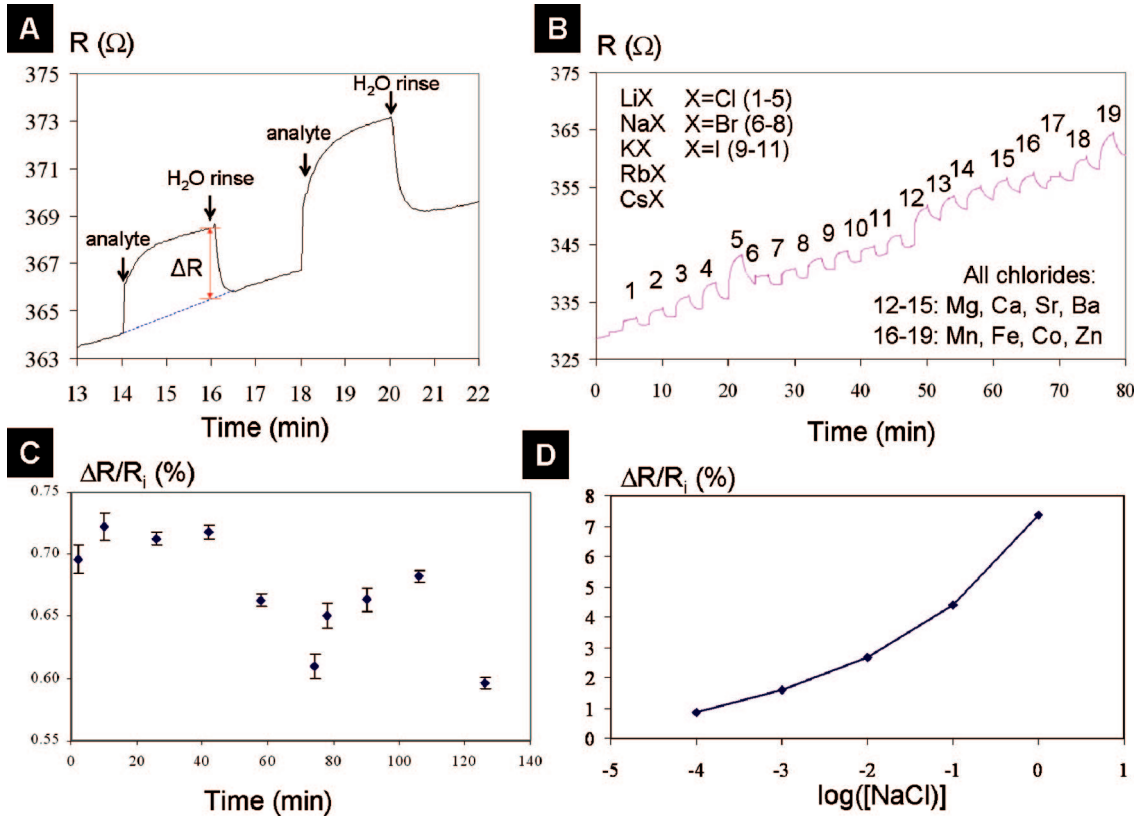


**Figure 2.** (A) Resistance of $LiMo_3Se_3$ nanowire film due to addition of 1.0 mM KCl (14 min) and 1.0 mM RbCl (18 min). (B) Resistance measurements of multiple analytes over an 80 min period. (C) Response of $LiMo_3Se_3$ nanowire film due to additions of 1.0 mM NaCl over a 130 min period. Error bars indicate uncertainties in determining $\Delta R$ values. (D) Response of $LiMo_3Se_3$ nanowire film as a function of NaCl concentration.

that are ~3−7 nm thick, according to TEM data (Figure 1B). Taking the crystallographic diameter of a single $LiMo_3Se_3$ nanowire as reference (0.85 nm), and assuming hexagonal close packing, each bundle consists of 12−48 individual $LiMo_3Se_3$ nanowires.

Sensors were fabricated by drop-coating dilute aqueous nanowire solutions onto indium tin oxide (ITO) electrode arrays followed by drying in a $N_2$ atmosphere. This produces circular films that are relatively even in thickness (Figure 1E), except for a nearly empty circular region near the center of the film and a thick rim at the film periphery. To restrict the charge transport across the 0.34 nm wide nonconductive gap (dotted line) to homogeneous areas of the film, the top and bottom edges of the films were removed with a razor blade. Even though the films appear to have a concentric structure, the nanowire orientation in the films is random, except for microdomains in which the bundles are partially aligned (see SEM and AFM micrographs in Figure 1C and D). The space between the nanowire bundles is well suited for analyte permeation.

Nanowire films prepared this way are not mechanically robust enough to withstand the convection forces during application of the analyte solutions. To improve mechanical stability, films were treated with a 20% KBr solution, followed by rising with water and drying in vacuo. As can be seen from the energy dispersive spectra in Figure S1 of the Supporting Information, this procedure results in exchange of the $Li^+$ ions with $K^+$ ions. The film composition after this treatment is $Li_{0.64}K_{0.36}Mo_3Se_3$. Films treated in this way do not degrade mechanically upon multiple applications of aqueous analyte solutions. We hypothesize that the increase in mechanical stability is due to the insolubility of the formed $KMo_3Se_3$ nanowire bundles in water.[27] In addition, potassium mediated cross-linkage among different bundles may occur.

Films prepared in this way (for simplicity, we refer to them as $LiMo_3Se_3$ hereafter) and mounted on the ITO electrode array give rise to an initial electrical resistance of ~200 Ω, as determined by two probe measurement. Application of water to the nanowire film leads to an increase of the resistance by about 10% (data not shown). We have previously shown that this is due to a swelling of the film caused by coating of the nanowires with the solvent.[18] Once the film resistance reaches a stable value, dilute (<1 mM) analyte solutions are sequentially applied to the films, with intermediate rinsing with water. This produces the temporal resistance changes as shown in Figure 2A. Upon addition of 1.0 mM KCl, the resistance increases quickly at first and then steadily. When the film is rinsed with water, the film resistance returns to the lower resistance value $R_i$. A similar curve also appears for RbCl. The observed sawtooth pattern is typical of sensors whose response is limited by the kinetics of analyte adsorption.[29] The fact that the signal is positive shows that ionic conduction of the analyte solution does not play a significant role. We note though that, for higher analyte concentrations (>1 mM), ionic conduction becomes important, as observed by a reduction of the resistance of the sensor (not shown). During sequential measurements, the resistance baseline $R_i$ (dashed blue line) has a positive, steady drift of approximately + 35 Ω/h during the first few hours, which we attribute to air oxidation of the nanowire film.[27,28,30] However, repeated

(29) Sotzing, G. A.; Briglin, S. M.; Grubbs, R. H.; Lewis, N. S. *Anal. Chem.* **2000**, *72*(14), 3181–3190.

(30) Heidelberg, A.; Bloess, H.; Schultze, J. W.; Booth, C. J.; Samulski, E. T.; Boland, J. J. *Z. Phys. Chem.* **2003**, *217*(5), 573–585.

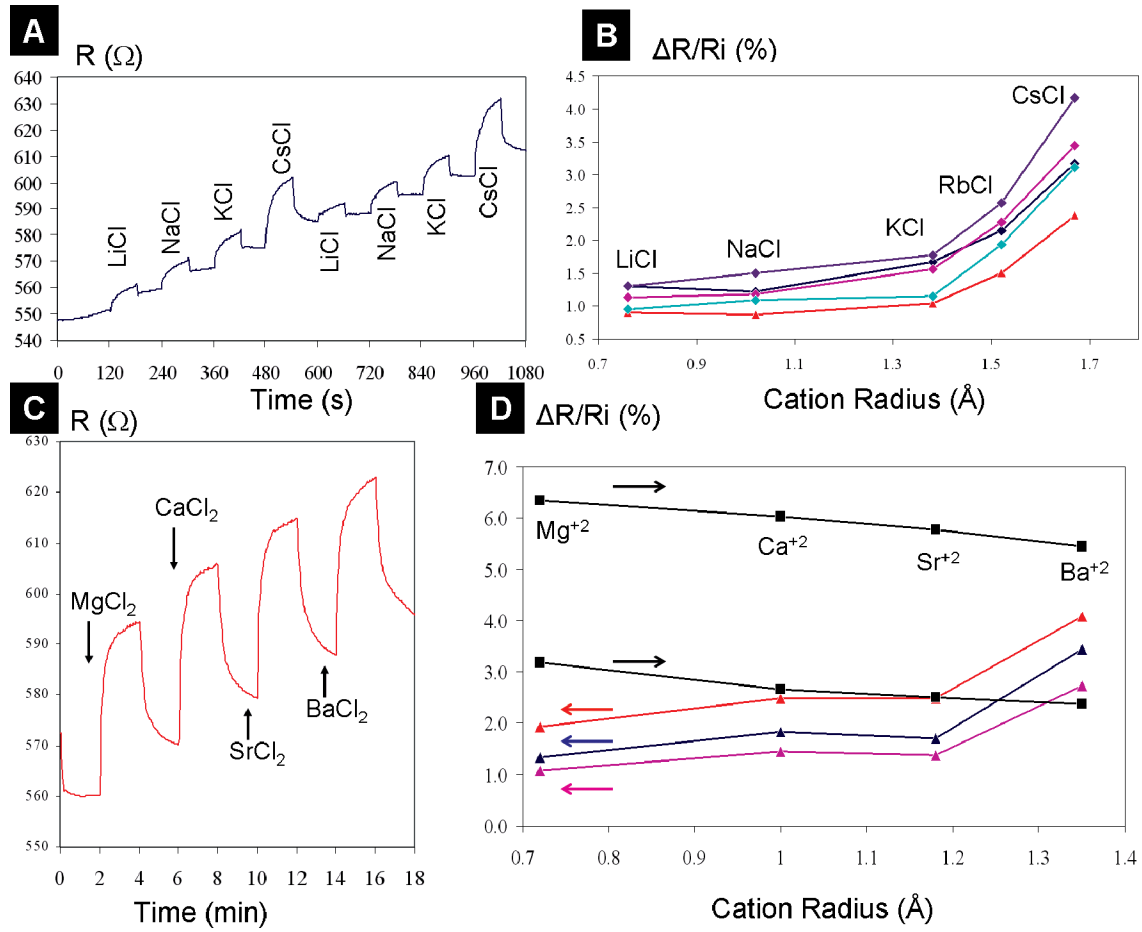


**Figure 3.** $LiMo_3Se_3$ nanowire film response to monovalent (A,B) and divalent cations (C,D). Arrows in (D) indicate order of analyte addition.

measurements with 1.0 mM NaCl over the course of 2 h (Figure 2B and C) show that reproducible data can be obtained within 30 min of exposing a film to air. For this period, the $\Delta R/R_i$ responses have a standard deviation of less than 2% of the mean $\Delta R/R_i$ value (Figure 2C).

At later times, the $\Delta R/R_i$ values become less reproducible and somewhat smaller. Besides time, the sensor response is also affected by the ITO electrode spacing, by the film thickness, and by the film width as described earlier.[18] To ensure reproducibility of the measurements, all films used in this study were prepared on the same electrode array and from a single nanowire stock solution. To compare values among different films, each resistance response is expressed as a percentage of the initial baseline resistance $R_i$ before analyte addition ($\%\Delta R/R_i$).

To test the concentration dependence of the sensor, nanowire films were exposed to NaCl solutions of variable concentration. The relative resistance changes of one film are plotted in Figure 2D. The resistance data shows a near-logarithmic dependence on the concentration, as expected for Langmuir adsorption behavior. However, the data cannot be fitted with a single adsorption constant, suggesting a variety of several different cation binding sites with different binding constants. Ion screening effects at higher concentrations, which reduce the effective cation charge, felt at the nanowires could also be responsible for the observed behavior. Nonlinear concentration−signal dependence has been previously observed for field effect transistor (FET) devices[7] and for Pd nanowire sensors.[13]

In order to determine the factors that govern the response of the $LiMo_3Se_3$ nanowire sensors, systematic tests of metal salts with variable metal cation oxidation states, cation and anion sizes, and hardness/softness were performed. For each set of measurements, the analyte concentration was 1.0 mM and the anion was held constant. Typical resistance−time traces for a series of alkaline metal chlorides are shown in Figure 3A. It can be seen that the $\Delta R/R_i$ response increases in the order of $Li^+ < Na^+ < K^+ < Rb^+ < Cs^+$. A plot of $\Delta R/R_i$ against the cation size is monotonic but not linear (Figure 3B). This trend is fully reproduced in seven sensors that were tested, even though absolute values of the response varied due to small differences in film morphology. Tests repeated for the same set of metal bromides revealed a similar trend, although $Li^+$ and $Na^+$ are less well differentiated by the sensor (Figure S2 in the Supporting Information). Reasons for the cation-size dependency of the sensor response are discussed below.

The response of the sensor to a series of alkaline earth metal halides at 1.0 M concentration is shown in Figure 3C. Compared to the group 1 metal salts, the group 2 metal salts are less easily removed from the sensor and require longer rinsing periods (3 min instead of 1 min) to bring down the resistance to the base resistance. Overall, the sensor responses are also less reproducible, and the resistance changes depend on the order of analyte addition. If the salts are tested in sequence of increasing cation size, a downward trend is observed in the resistance−size data (Figure 3D). If the salts are tested in reverse order, there is an upward trend in the data. This indicates that the metal ions undergo irreversible adsorption, which can be explained with the higher charge of the cations that increases the coulomb interactions with the negatively charged nanowires. Considering that the slopes of the forward and backward graphs are about equal in magnitude,

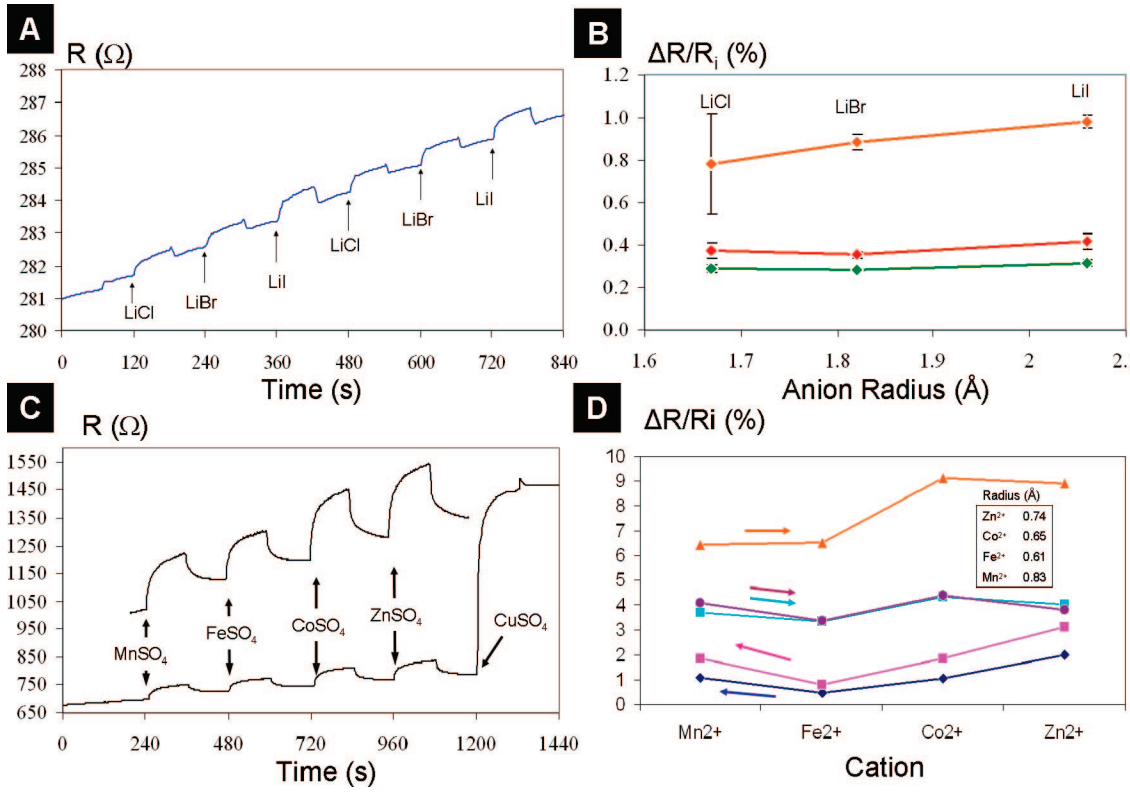


**Figure 4.** (A) Resistance traces of the sensor in response to LiX (X = Cl, Br, I). (B) Plot of sensor response versus anion radius (Cl, Br, I). Error bars indicate standard deviation of three separate measurements. (C) Resistance traces caused by first row transition metal ions (inset shows magnified bottom trace). (D) Plot of $\Delta R/R_i$ versus transition metal cation. Arrows indicate the sequence of analyte addition. The inset lists cation radii.

it seems reasonable to assume that the observed resistance trends can be solely attributed to irreversible adsorption effects. One can therefore conclude that there is no size-specific sensor response for the group 2 metal cations, in contrast to the case of the group 1 metal cations.

In order to examine the sensitivity of the sensors toward anions, nanowire films were sequentially exposed to equal concentrations (1.0 mM) of alkali metal chlorides, bromides, and iodides. For the lithium salts, no significant differences in $\Delta R/R_i$ values were observed for the three anions as can be seen in Figure 4A and B. For the sodium and potassium salts MX (M = Na, K; X = Cl, Br, I), also no significant effect of the anion (Figure S3 in the Supporting Information) was observed, except for one film which showed a small decrease of $\Delta R/R_i$ with increasing anion size. Overall, these measurements revealed that there is no relationship between anion size and film response. This is consistent with a model in which only the metal cation is able to interact with the negatively charged nanowire bundles, whereas the anions are repelled because of their negative charge.

Nanowire films also detect ions from the first transition metal series. For these experiments, the relatively low redox potential of $LiMo_3Se_3$ of +0.74 V vs NHE has to be taken into consideration, which makes the nanowires prone to oxidation.[17] This effect is shown for $CuSO_4$ in Figure 4C. This analyte leads to a strong but irreversible resistance increase of the nanowire film, owing to oxidation of the nanowires. The reduction potential of the $Cu^{2+/0}$ redox couple (+0.34 V vs NHE)[31] is much lower than the $LiMo_3Se_3$ oxidation potential, but the interaction of the reaction product with the nanowires can increase the potential. The other tested ions ($Mn^{2+}$, $Fe^{2+}$, $Co^{2+}$, $Zn^{2+}$) had lower redox potentials and did not oxidize the nanowire. However, as for the group 2 metal cations, irreversible adsorption effects again play a role, requiring rinsing times of ≥2 min (Figure 4C). To determine the reversibility of the sensor response toward these ions, analyte additions were performed in two opposing directions as shown by the arrows in Figure 4D. Again, the sensor response becomes weaker with each sequential ion addition, indicating irreversible adsorption of the ions. Regardless of the addition order, $Fe^{2+}$ ions give small $\Delta R/R_i$ values, which correlates with the fact that $Fe^{2+}$ ions also have the smallest ion radius in the series (see inset of Figure 4D for values). Thus, it seems that, in contrast to the group 2 metals, ion size is a significant factor with the transition metals.

Overall, the responses of the transition metal cations are about 4−6 times larger than those of the monovalent cations of group 1 (Figure 3B). In order to determine if there is a correlation of the signal with the cation charge, a single nanowire film was alternately exposed to group 1 and group 2 metal salts, as shown in Figure 5A and B. For the couples $Na^+/Mg^{2+}$ and $K^+/Ca^{2+}$, the divalent ion gives the larger response, while for the couple $Cs^+/Ba^{2+}$ the responses are the same (Figure S4 in the Supporting Information). This clearly establishes charge as a factor for the smaller ions from the third and fourth period in the periodic table. For the couple $Cs^+/Ba^{2+}$, this correlation breaks down, mainly because $Cs^+$ gives such a strong response (Figure 5C).

Finally, the responses of all measured ions are plotted in one common diagram against cation radii (Figure 5D). To allow this direct comparison, signals from different sensors were scaled using NaCl as a standard. Strong responses are observed for divalent cations, due to their higher charge. Among these ions, there are no distinctive size trends, except for the smallest divalent cation $Fe^{2+}$, which also produces the weakest response of all divalent cations. For the monovalent group elements, there is a strong correlation between sensor response and cation size. Here,

(31) Weast, R. C. *CRC Handbook of Chemistry and Physics*, 87th ed.; CRC Press: Boca Raton, FL, 2006.

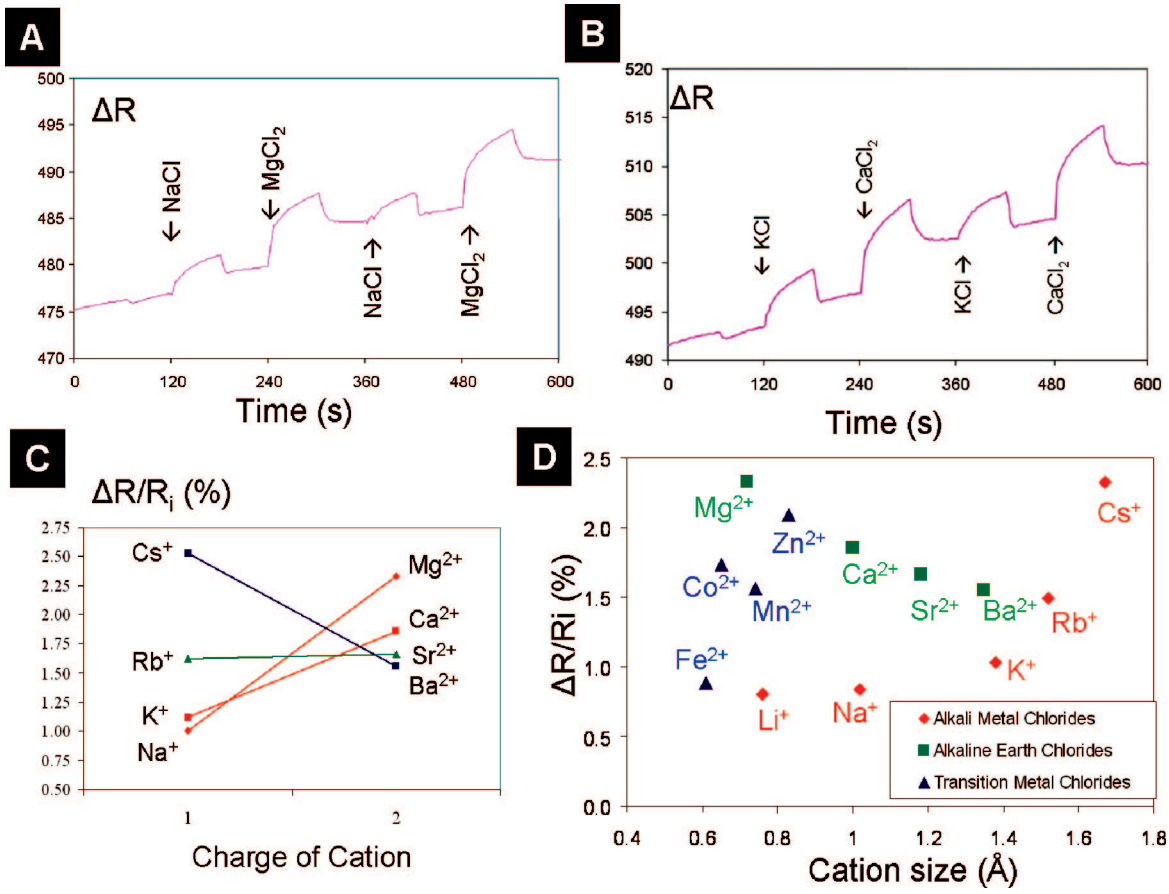


**Figure 5.** (A) Resistance change for NaCl versus $MgCl_2$. (B) Resistance change for KCl versus $CaCl_2$. (C) Comparison of $\Delta R/R_i$ values for mono- and divalent ions. (D) Comparison of the responses of all cations. A NaCl standard was employed to scale responses obtained from different nanowire films.

the $\Delta R/R_i$ values monotonically increase with increasing cation radius.

The fact that the sensors discriminate size only for the monovalent ions but not for the divalent ions suggests that there is an intrinsic difference in the sensing mechanism for these species. It also implies direct contact between the metal ions and the nanowires, at least for the group 1 cations. For the interaction, there are two options. First, the cations $M^+$ might exchange in the nanowire bundles, producing the known phases $MMo_3Se_3$ (M = Li, Na, K, R, Cs).[28,32] The observed resistance changes would then be due to the different intrinsic conductivities of these phases. If cation exchange were to occur, the resistance of the films could not decrease by simply rinsing the nanowire films with water, which is what is observed. The other, more likely option is that cations adsorb to the surface of the nanowires, owing to attractive electrostatic interactions between these species. The strong observed responses for $Rb^+$ and $Cs^+$ could then be explained with the greater binding affinity of these *softer* cations to the *soft* selenide in $LiMo_3Se_3$.

Another question concerns the mechanism by which the adsorbed cations reduce the electrical conductance of the nanowire films. First, it is possible that the cations assert a field effect on the nanowires, causing them to function as ion-selective field effect transistors (ISFETs).[1,33,34] Based on preliminary gated conductance measurements, we rule out this possibility. Nanowire films mounted on an insulator-coated gold substrate exhibit ohmic behavior, and their electrical conductance is fully independent from the gate voltage, which was varied from −5.0 to + 5.0 V (Figure S5 in the Supporting Information). A second possibility is that ionic analytes either raise or diminish the energetic barrier for interwire charge transport, similar to what has been postulated for $LiMo_3Se_3$ nanowire films during the detection of molecular vapors.[16] While we cannot rule out this possibility, it would appear that negatively charged ions should have the opposite effect of positively charged ions. Instead, the data suggests that anions do have a negligible effect on charge transport in the nanowire films. The final possibility is that the metal ions act as scattering centers for conduction electrons in the nanowire bundles. Scattering of conduction electrons has been made responsible for the positive resistance change observed for thin metal (gold, silver, copper) films or wires in contact with molecular adsorbates.[35–39] In such structures, conduction is limited by electron scattering because at least one structural dimension is smaller than the mean free path of the electrons. Upon analyte adsorption, the electrical resistance increases 3−5% of the base resistance. The magnitude of the change and its sign agree with our observations, suggesting a similar mechanism for $LiMo_3Se_3$ nanowire films.

(32) Song, J. H.; Messer, B.; Wu, Y. Y.; Kind, H.; Yang, P. D. *J. Am. Chem. Soc.* **2001**, *123*(39), 9714–9715.
(33) Schoning, M. J.; Poghossian, A. *Analyst* **2002**, *127*(9), 1137–1151.
(34) Bergveld, P. *IEEE Trans. Biomed. Eng.* **1970**, *BM17*(1), 70.
(35) Coutts, T. J. *Thin Solid Films* **1971**, *7*(2), 77.
(36) Liu, Z.; Searson, P. C. *J. Phys. Chem. B* **2006**, *110*(9), 4318–4322.
(37) Sondheimer, E. H. *Adv. Phys.* **2001**, *50*(6), 499–537.
(38) Greene, R. F; Odonnell, R. W. *Phys. Rev.* **1966**, *147*(2), 599.
(39) Hein, M.; Schumacher, D. *J. Phys. D: Appl. Phys.* **1995**, *28*(9), 1937–1941.

## Conclusion

In summary, we have carried out the first systematic investigation of electrical metal ion detection by metallic nanowire films. Ions from group 1, group 2, and several first row transition elements can be directly detected in solution with an increase of the nanowire film resistance that occurs over a 30−240 s period. Negatively charged ions are not detected. For metal cations, the sensor response depends on the ion charge, and for the group 1 cations it depends also on ion size, which we attribute to the softer character and stronger binding affinity of the larger group 1 elements to the nanowires. The response is also exponentially dependent on the analyte concentration, suggesting that there is more than just one type of analyte adsorption site in the film. The magnitude of the resistance changes and their direction are in agreement with an electron scattering model as discussed above.

**Acknowledgment.** This research was supported by NSF Grant CTS-0427418.

**Supporting Information Available:** Elemental composition data for $LiMo_3Se_3$ films, additional temporal resistance plots for group 1 and 2 halides, and gated conductance data for $LiMo_3Se_3$ films. This material is available free of charge via the Internet at http://pubs.acs.org.

LA8004085